sciendo

DOI 10.2478/ama-2024-0026

acta mechanica et automatica, vol.18 no.2 (2024)

ASSESSMENT OF PARAMETERS OF THE VIBRATION-BASED ENERGY HARVESTING SYSTEM LOCATED IN THE MICRO-POWER GENERATOR

Andrzej KOSZEWNIK*

*Faculty of Mechanical Engineering, Bialystok University of Technology, Wiejska 45C Street, 15-351 Białystok, Poland

a.koszewnik@pb.edu.pl

received 7 April 2023, revised 8 September 2023, accepted 17 September 2023

Abstract: This article presents the optimisation process of some key parameters such as the size of the macro-fibre composite (MFC) and the optimal impedance load matching the piezoelectric harvester located in the prototype of the micro-power generator to enhance the vibration-based energy harvesting effect. For this, the distributed parameter model of this structure, including MFCs of the 8514 P2, 5628 P2 and 8528 P2 types, with a homogenous material in the piezoelectric fibre layer was determined. The numerical analysis of the FEM model of the flexure strip with piezo-composite indicated that the highest amplitude of voltage >7 V is generated by the proposed device with the piezo of the 8528 P2 type, while the lowest amplitude (close to 1.1 V) was noted for the piezo of the 8514 P2 type. Experiments were carried out on the laboratory stand to verify the obtained results. In addition, it was shown that the power output of the real EH system with the piezo of the MFC 8528 type, connecting with the matched resistive load (R = 120 kΩ), led to a significant increase in the value of the generating voltage up to 500 mW versus EH system with the piezo of 8514 P2 and 5628 P2 types. Finally, the effectiveness of this system was found to be close to 33% for the EH system with the piezo of the 8528 P2 type.

Key words: macro-fibre composite, homogenised material, micro-piezo generator, vibration-based energy harvesting system

1. INTRODUCTION

Energy harvesting is defined as the direct conversion of unused ambient energy, such as mechanical, thermal and solar, to electrical energy. The most popular and generally known energy harvesting methods in civil infrastructure are solar panels or wind turbines, which powers electronic devices with a high power demand. Another approach is using vibration-based energy harvesters that utilise vibrations of a mechanical structure or ambient vibrations that can be used to power small-scale sensors and actuators of a low power demand.

Numerous methods of converting mechanical motions to electric energy from a technical point of view, such as piezoelectric [1–3], electrostatic [4], and magnetostrictive or electromagnetic energy [5], can be found in the literature. Among them, piezoelectric generators is the most efficient in such applications due to their simple structure and the high robustness to external/internal electromagnetic waves. In addition, the effectiveness of this type of generator can be improved by modifying the piezoelectric materials, changing the stress direction, or altering the electrode pattern. Unfortunately, apart from these advantages, piezoelectric generators have numerous disadvantages, such as depolarisation, poor coupling in the piezo-film and poor adhesion between the polyvinylidene fluoride (PVDF) film and electrode material [6,7].

A group of researchers, with Morita as a leader, showed that electromagnetic energy harvester generators have a high energy density and they can be fabricated without any difficulties [8]. Compared to piezoelectric generators, smart materials and external voltage sources are not needed for electromagnetic generators. Hence, Nicoleti pointed out that electromagnetic harvesters represent a low-cost solution with the possibility of operating without any contact with the vibrating structure [9]. Similar to piezo generators, electromagnetic generators also have numerous disadvantages, one of which is the fact of being affected by electromagnetic waves, which will pose some difficulties when integrating with MEMS [10].

Smart materials are not needed for electrostatic generators, and they are also compatible with MEMS [11]. The advantages of electrostatic generators are presented in an article written by Roundy [12], who pointed out that using the out-of-plane gap-closing convert method will yield the highest potential capacitance, and the interaction between the two planes makes them easy to stick together. Other advantages of this method are described in articles [13,14] written by Li et al., who showed that an electrostatic MEMS energy harvester with a novel non-uniform comb or impact-based frequency up-conversion can enhance the power output generated by this device. Similar results were also obtained in a previous study [15] where an electret-based Vibration Energy Harveters (e-VEH) device with the frequency up-conversion was used.

Electrostatic generators are widely used in many applications because of the advantageous properties of the piezo-patch strips and piezo-stacks [16–20]. Here is an example of such an application in structural health monitoring (SHM): [21] Pakrashi et al assessed the leak localisation in water pipes using piezo-patches and investigated several pipes with different widths of leak to propose and calibrate a leak index based on the monitoring voltage from a piezoelectric energy harvester (PEH) and the power spectrum of the output signal generated from particular PVDF piezoelectric transducers. Similar experiments have been carried

DOI 10.2478/ama-2024-0026

out for bridge monitoring under operational conditions via Pb-zirconate titanate (PZT) patches [18,22,23] or the damage identification metric for smart beams with macro-fibre composite (MFC) elements to support SHM [24]. Ambroziak et al. [25] used piezoelectric energy harvesting systems for monitoring the propulsion system of Vertical Take-off Landing Unmanned Aerial Vehicle (VTOL UAV) in their study, where they investigated healthy and damaged propulsion systems and proposed a methodology for quickly detecting the failure of the UAV propulsion system.

As mentioned earlier, piezoelectric energy harvesting systems are also used to improve the effectiveness of systems, especially in a low frequency range. Pan et al. designed a hybrid energy harvester [26] that can generate an output power close to 70 μW. A similar study was done by Yang et al. who used a rail-borne PEH to collect energy from random railway vibrations [27]. They also demonstrated that the output power peaks from the system at the first two resonance frequencies are close to 10 mW. In another study [28], Wu et al. proposed a while-drilling energy harvesting device as a continuous power supply for downhole instruments during the drilling procedure. The designed device can obtain the best energy harvest performance with a peak voltage of 20–40 V and with the thickness of piezo-strips of 1.2–1.4 mm. Kan et al. [29] developed a PEH excited by an axially pushed wedge cam. The proposed rotary energy harvester is characterised by the simultaneous realisation of unidirectional deformation and limited amplitude for piezoelectric vibrations. Under the optimum matching parameters, the proposed harvester generated a maximum power of 10 mW. Ju et al. [30] proposed an energy harvester that consists of spherical proof mass in an aluminium housing and a piezoelectric cantilever beam fabricated by attaching metal blocks at the free end of an MFC beam. The obtained experimental results indicated that the proposed harvester based on an indirect impact enhanced the energy harvesting effect by obtaining an average power output of 964 μW by 3 g acceleration at 18 Hz.

The effectiveness of the energy harvesting system for cantilever beam structures can be also enhanced by considering the broadband effect. For example, Zhou et al. [31] used a novel multi-mode intermediate beam with a tip mass called a “dynamic magnifier”. The results of in this study showed that the amplitude of the voltage generated by the proposed harvester in a low frequency range significantly increased in comparison to the conventional energy harvesting system. Similar results were obtained in a study by Caban et al. [32], where an energy harvesting system was located on a diesel engine suspension.

Other devices that produced more amount of energy are piezo generators equipped with piezo-stacks. For example, Peng et al. [33] indicated that this kind of generator can produce an instantaneous peak power of 300 mW. Similarly, Wen et al. [34] designed a piezoelectric generator with an integrated multistage force application. The experimental results showed that a high-peak power output of 50 mW can be obtained from the proposed device when connected with a properly matched resistive load.

Regardless of the type of piezoelectric generators, their effectiveness, especially in a low frequency range, can be enhanced by connecting them with storing units containing supercapacitors or the synchronised switch harvester on inductor (SSHI) circuit [35–39]. For example, Selleri et al. [40] described a system composed of an ionic liquid-based supercapacitor and a PZT disc. The charging process of the aforementioned supercapacitor, which lasted 2 h, lighted an LED for 120 s. Similarly, Koszewnik et al. [41] used an SSHI circuit in a beam-slider structure with an MFC composite to obtain an amplitude of voltage output of >20 V.

Taking the presented peer review into account, this study focuses on overcoming the problem of generating voltage from vibration-based systems with a low amplitude. To this end, the micro-power piezoelectric generator with MFC films attached to the host structure is designed and tested. In addition, in the proposed generator, the MFC made of a homogenised material in the active layer of the piezo is considered to show a novelty in the power range of some low-energy sensors. This article is organised as follows. The electromechanical model of the piezo harvester located on the considered mechanical structure in physical and modal coordinates is described in Section 2. In Section 3, the computational models of all structures with a homogenous model of MFC, which is also a core novelty of this study, is presented. Next, in Section 4, experimental investigations for three different host structures of the generator with MFC films of the 8514 P2, 5628 P2 and 8528 P2 types are presented and described. In addition, the effectiveness of the proposed energy harvesting system is assessed in this section. Section 5 concludes the main findings of this work.

2. ELECTROMECHANICAL MODEL OF THE ENERGY PIEZO HARVESTER LOCATED IN THE PROTOTYPE OF THE MICRO-POWER GENERATOR

In this section, a brief description of an electromechanical model distributed parameters of a flexure strip with a piezo-patch being part of the proposed prototype of the micro-power generator is analysed. To this end, the fixed–fixed glass fibre beam, being the host structure of the generator, is equipped with one piezo-strip harvester MFC including a single active layer, two Kapton layers and two electrode layers. As a result, a smart structure of the generator is designed, shown in Fig. 1. The parameters of the host beam, as well as the piezo adjusted to its structure, are listed in Tab. 1.

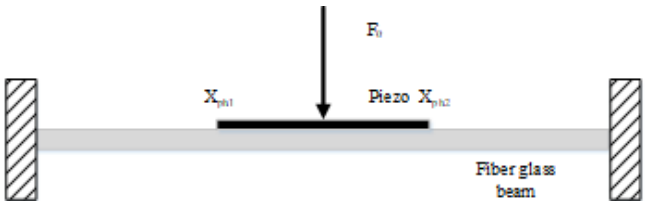

Fig. 1. Simplified model of a fixed–fixed beam with the piezo-strip

As can be seen in Fig. 1, a fixed–fixed beam representing the flexure strip of a micro-power generator with an integrated harvester is excited to vibration by force F_0 deriving in a real structure from the vibration shaker by the pusher and the cross-amplifying mechanism. The mentioned piezo-composite of the length of L_P, the width of w_P and the thickness t_P of the whole MFC, integrated with the host structure at the position x_{PH1}, $x_{PH2,}$ was used to measure voltage from the vibration structure.

Then, the general equation of the transverse vibration of such excited part of the generator can be expressed as follows:

$$[E_F I_F + E_P I_P (H(x - x_{PH2}) - H(x - x_{PH1}))] \frac{\partial^4 w(x,t)}{\partial x^4} + [m_F + m_P (H(x - x_{PH2}) - H(x - x_{PH1}))] \frac{\partial^2 w(x,t)}{dt^2} + -\Gamma V(t) \left[\frac{d\,\partial(x - x_{PH2})}{dx} - \frac{d\,\partial(x - x_{PH1})}{dx} \right] = F_0 \delta(x - x_0) \quad (1)$$

where: E_F is Young's modulus of the flexure strip of the generator, E_P is Young modulus of the piezo-composite harvester element, I_F is the inertia moment of the flexure strip, I_P is the inertia moment of the piezo-composite harvester element, m_F is the mass per unit length of the flexure strip, m_P is the mass per unit length of the piezo-composite harvester, $H(x)$ is the Heaviside function, $\delta(x)$ is the Dirac function along the longitudinal direction, $V(t)$ is the voltage flowing through the external resistive load R, F_0 is the force obtained from the pusher and the cross-amplifying mechanism of the micro-power generator, $x_{\_PH1}$ is the initial location of the piezo-patch harvester on the host structure, $x_{\_PH2}$ is the ending location of the piezo-patch and Γ is the electromechanical coupling factor.

Tab. 1. Parameters of the host structure and three different piezo-patch composites MFC 5628, MFC 8514 and MFC 8528 [15]

Mechanical parameters								
Fibre glass								
Length [mm]	Width [mm]	Length [mm]						
L_F 140	w_F 38	t_F 1 5						
Young's modulus (GPa)	Poisson's ratio (-)	Density [kg/m3]						
E_F 80	v_F 0.22	ρ_F 2,600						
Piezo-composite MFC								
Young's modulus (GPa)	Poisson's ratio (-)		Piezo-charge coeff. (pC/N)	Relative permittivity (-)				
E_x 31.6	v_{xy} 0.4		d_{31} −173	ε_r^T 2,253				
E_y 17.1	v_{yz} 0.2		d_{32} −150					
E_z 9.5	v_{xz} 0.4		d_{33} 325					
Geometrical parameters								
Overall length [mm]		Overall width [mm]		Active length [mm]	Active width [mm]	Thick. of PZT fibre layer [μm]	Thick. of electrode layer [μm]	Thick. of Kapton layer [μm]
L_p	103	w_P	31	85	28	180	25	30
	103		17	85	18	180	25	30
	67		31	56	28	180	25	30

MFC, macro-fibre composite; PZT, Pb-zirconate titanate.

The piezoelectric element used in the generator requires considering the approach from the electrical point of view. For this, the electrical charge accumulated at its electrodes can be calculated over the whole surface area in the following form:

$$\boldsymbol{Q} = \int_{\boldsymbol{x\_PH1}}^{\boldsymbol{x\_PH2}} \left(\boldsymbol{d_{31}E_P\bar{\delta}_P + \varepsilon_{33}E_3}\right)\boldsymbol{w_P dx} \tag{2}$$

where ε_{33} is the permittivity at constant stress, $\bar{\delta}_P$ is the bending strain along the middle surface of the piezo layer and E_3 is the electric field.

Next, applying Ohm's law, the current flowing through the load resistor R, connected to the MFC, can be expressed as follows:

$$\boldsymbol{i(t)} = \frac{\boldsymbol{V(t)}}{\boldsymbol{R}} = \frac{\boldsymbol{dQ}}{\boldsymbol{dt}} = \frac{\boldsymbol{d}}{\boldsymbol{dt}}\left[\int_{\boldsymbol{x\_PH1}}^{\boldsymbol{x\_PH2}} \left(\boldsymbol{d_{31}E_P\bar{\delta}_P + \varepsilon_{33}E_3}\right)\boldsymbol{w_P dx}\right]$$

where R is the resistive load applied to the system.

Taking Eq. (3) into account, it can be seen that the current $i(t)$ is strongly associated with strains of the piezoelectric harvester and the electrical field applied to its electrodes. This resulted in the fact that the electrical circuit of the system can be obtained by substituting the electric field $E_3 = -V(t)/t_P$ and the strain $\bar{\boldsymbol{\delta}}_{\boldsymbol{PH}} = -\boldsymbol{t_c}\frac{\boldsymbol{\partial^2 w}}{\boldsymbol{\partial x^2}}$ in the following form [16]:

$$C_p\frac{dV(t)}{dt} + \frac{V(t)}{R} + \Gamma\left[\int_{x\_PH1}^{x\_PH2}\frac{\partial^3 w(x,t)}{\partial x^2\,\partial t}dx\right] = 0 \tag{4}$$

where C_p is the capacitance of the piezo-patch harvester $C_p = \frac{\varepsilon_{33} w_P L_P}{t_P}$

Both equations Eqs (1) and (4) refer to distributed electro-elastic model parameters of the piezo-patch harvester integrated to a 1D mechanical structure in physical coordinates. However, from the energy harvesting point of view, it should be analysed in modal coordinates. For this purpose, vertical displacement of the beam as a host structure is represented as multiplication of an absolutely and uniformly convergent series of the eigenfunctions in the following form:

$$w(x,t) = \sum_{n=1}^{\infty}\varphi_n(x)\eta_n(t) \tag{5}$$

where $\varphi_n(x)$ is the mass normalised eigenfunction (mode shapes), $\eta_n(t)$ is the modal time response of the system for n-th mode.

The considered structure represents the fixed–fixed beam. As it was applied, the eigenvectors of this structure, after considering the boundary coordinates, given in Eq. (6), and split by geometric and time variables, can be expressed as given in the following equation [7]:

$$w(0,t) = 0 \qquad w(L_F,t) = 0$$
$$\left.\frac{\partial w(x,t)}{\partial x}\right|_{x=0} = 0 \qquad \left.\frac{\partial w(x,t)}{\partial x}\right|_{x=L_F} = 0 \tag{6}$$

$$\phi_n(x) = \left(\cosh(\lambda_n L_F) - \cos(\lambda_n L_F)\right)\left(\cosh\left(\frac{\lambda_n}{L_F}\right)x - \cos\left(\frac{\lambda_n}{L_F}\right)x\right) + -\left(\sinh(\lambda_n L_F) + \sin(\lambda_n L_F)\right)\left(\sinh\left(\frac{\lambda_n}{L_F}\right)x + \sin\left(\frac{\lambda_n}{L_F}\right)x\right) \tag{7}$$

where $\lambda_n = \frac{(2n+1)\pi}{2\cdot L_F}$ for n = 1,2. λ_n is the frequency parameter of an undamped host structure.

Substituting Eq. (7) into Eq. (1) leads to solving the eigenvalue problem of the smart beam for short circuit conditions. Then, the natural frequency ωn of the structure, with no piezoelectric patch for the n-th mode, can be presented in the following form:

$$\omega_n = \lambda_n^2\sqrt{\frac{E_F I_F}{m_F {L_F}^4}} \tag{8}$$

where LF is the length of the flexure strip of the micro-power generator.

DOI 10.2478/ama-2024-0026

Taking account of the modal analysis procedure of the 1D structure with a piezo harvester adjusted to its surface by using support, an electromechanical coupled ordinary differential equation for the modal time response $\eta_n$can be expressed as follows [7]:

$$\frac{d^2\eta_n(t)}{dt^2} + 2\xi_n\omega_n\frac{d\eta_n(t)}{dt} + \omega^2{}_n\eta_n(t) + \tilde{\Gamma}_n V(t) = f_n(t)\delta(x - x_0) \quad (9)$$

where ξ_n is the modal damping ratio, $f_n(t)$ is the modal force applied to the structure.

As a result, the modal electromechanical coupling term $\tilde{\Gamma}_n$can be presented as follows:

$$\tilde{\Gamma}_n = -E_P d_{31} w_P t_c \int_{x\_PH1}^{x\_PH2} \frac{d^2\varphi_n(x)}{dx^2} dx = -E_P d_{31} w_P t_c \frac{d\varphi_n(x)}{dx}\Big|_{x\_PH1}^{x\_PH2} \quad (10)$$

The obtained modal electromechanical coupling term given by Eq. (10) and the vertical deflection from Eq. (7) put into Eq. (4) lead to modifying the electrical circuit equation in the following form:

$$\boldsymbol{C_p}\frac{\boldsymbol{dV(t)}}{\boldsymbol{dt}} + \frac{\boldsymbol{V(t)}}{\boldsymbol{R}} - \sum_{\boldsymbol{n=1}}^{\infty}\tilde{\boldsymbol{\Gamma}}_{\boldsymbol{n}}\frac{\boldsymbol{d\eta_n(t)}}{\boldsymbol{dt}} = \boldsymbol{0} \quad (11)$$

The performed considerations of the tested structure with different active areas of the integrated piezo-patch harvester for modal coordinates allow to assess the voltage generated by the piezo as well as the effectiveness of the proposed Energy Harvester (EH) system located in the micro-power generator.

3. PROTOTYPE OF THE MICRO-POWER GENERATOR

The proposed micro-power generator with an EH system located on the flexure strip is shown in Fig. 2. It consists of a telescoping rod (1), cover (2), body case (3), cross-amplifying mechanism (8), flexure strip (5) and MFC piezo-strip (9). All elements, apart from the telescoping rod, were printed using a 3D printer and PLA filament wire of 1.75 mm diameter developed by Fiberlogy company. In addition, from the mechanical point of view, bearing balls are used to eliminate frication in the cross-amplifying mechanism.

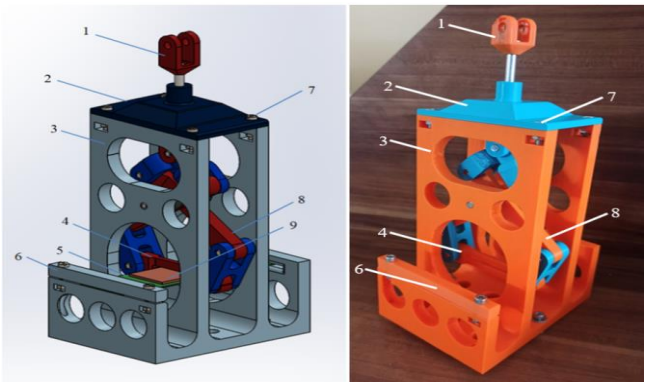

Fig. 2. Numerical model and prototype of the piezoelectric generator

3.1. Finite Element Model (FE) of the piezo generator and numerical results

The process of assessing parameters of the energy harvesting system in the micro-piezo generator is described in this section. In addition, the numerical calculations of the micro-piezo generator, including the flexure strip of a length of 140 mm, a width of 38 mm and a thickness of 1 mm and three different piezo-patch harvesters (MFC 5628, MFC 8514 and MFC 8528), are made.

To determine the parameters of the energy harvesting system located in the micro-piezo generator, the finite element (FE) model of the whole generator designed in Ansys is used. Taking this into account, the flexure strip structure made from glass fibre is modelled using an 8-node coupled-brick element Solid186, while the MFC element is discretised by using the representantive volume elements (RVE) technique [24,43]. Then, according to this method, the piezoelectric fibre layer with a homogenised material is modelled using a Solid 226-node coupled brick element, while the electrode and Kapton layers of the harvester are modelled using an 8-node coupled-brick element, Solid186. As a result, the computational model of the considered structure is determined, shown in Fig. 3b, where the thickness of the adhesive layer (<15 μm) is omitted.

(a)

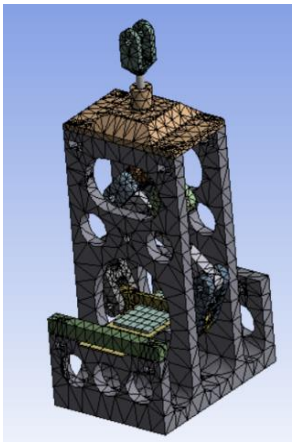

(b)

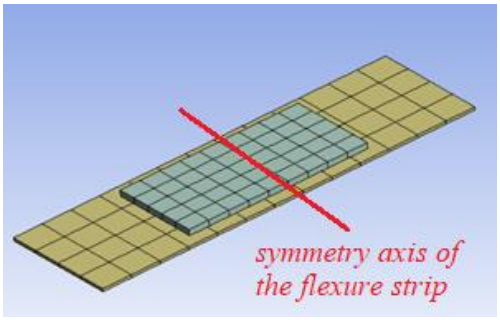

Fig. 3. Computational model (a) of the whole micro-piezo generator, (b) the flexure strip with piezo

Next, the behaviour of the flexure strip with the piezo element is analysed in the frequency domain. For this, a modal analysis of the FEM model of the proposed generator is performed in the limited frequency range of 1–300 Hz.

DOI 10.2478/ama-2024-0026

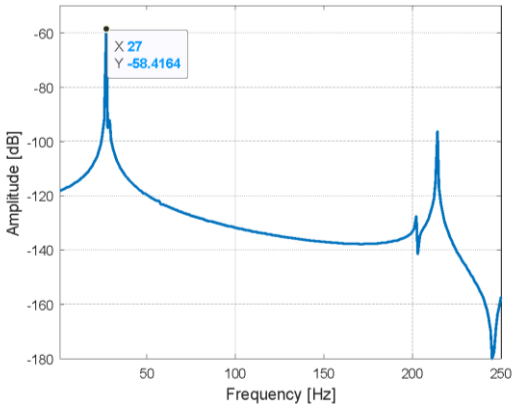

Fig. 4. Frequency response function of the FEM model of the flexure strip with chosen piezo-strip of type MFC 8514 P2

(a)

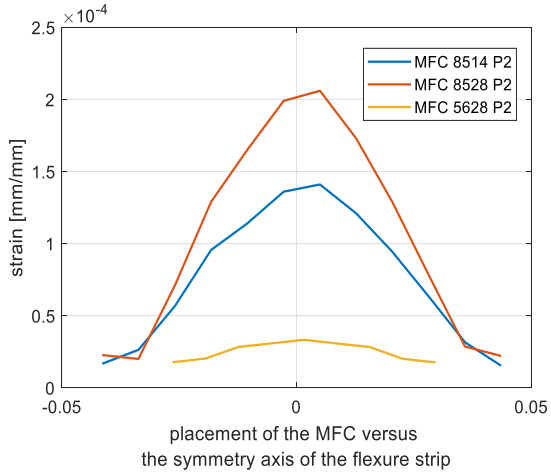

(b)

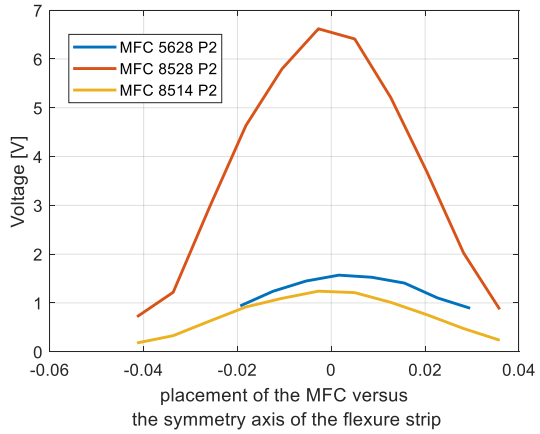

Fig. 5. Comparison of (a) strain distribution and (b) voltage generated by MFCs versus the symmetry axis of the flexure strip

Observing the determined amplitude plot of the flexure strip with a piezo-composite presented in Fig. 4, it can be noticed that this system should effectively work in the first resonance, where the amplitude peak is the highest. In the case of exciting the system to vibration with the second natural frequency, it can be supposed that the effectiveness of this system significantly decreases due to a smaller amplitude of strains of the piezo-composite. This behaviour allows to conclude that further analysis of this micro-piezo generator should be considered in the narrow frequency range, not exceeding 30 Hz.

Next, a harmonic analysis of this generator is performed to assess the parameters of the energy harvesting system located on the flexure strip according to Eq. (11). To do this, the computational models of the flexure strip with three different piezo-strips were excited to vibration by applying a sinusoidal excitation with a frequency close to the first natural frequency. The obtained results from the "Piezo and Mems Toolbox" (see Fig. 5) show that the size of the piezo-composite is a significant parameter that influences the values of strains, amplitude voltage output, as well as the effectiveness of the EH system.

As shown in Fig. 5b, the use of the piezo harvester with the highest active area (MFC 8528) leads to the generation of the highest amplitude strains and, consequently, the highest amplitude of voltages. In the case of using piezo-composites with the same length and twice shorter width (MFC 8514), smaller strains can be observed on the surface of this element and lower amplitudes of voltage generated by this element. A different effect is achieved for the piezo generator with the piezo-composite of the MFC 5628 type. In this case, shortening the length of the piezo-strip elements by the same width leads to generating a slightly higher voltage amplitude than that in the case of the piezo of the MFC 8514 type. This effect is due to the emergence of slightly higher strains in the longitudinal direction of this piezo.

4. EXPERIMENTAL SETUP

The process of the parameter assessment of the energy harvesting system located in the piezoelectric generator was carried out on the lab stand, as shown in Fig. 6, to verify the numerical results.

a)

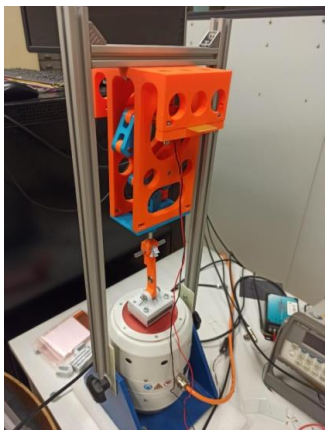

(b)

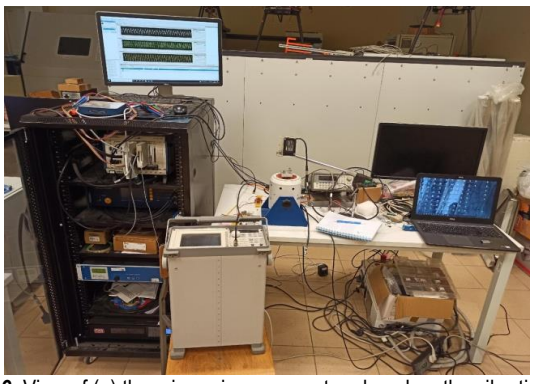

Fig. 6. View of (a) the micro-piezo generator placed on the vibration shaker Tira TV 51110-M, (b) the whole lab stand with the retrofitted equipment

DOI 10.2478/ama-2024-0026

To do this, three different MFCs of 8514 P2, MFC 5628 P2 and MFC 8528 P2 types composed of two Kapton layers, two epoxy layers and one PZT fibre layer were chosen for an experimental test, where each of them was attached to the fibreglass beam with an adhesive epoxy layer of the Uhu plus type. The parameters of the host structure are listed in Tab. 1.

(a)

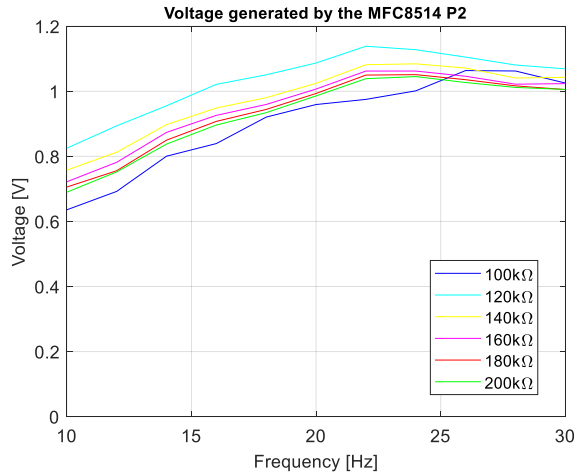

(b)

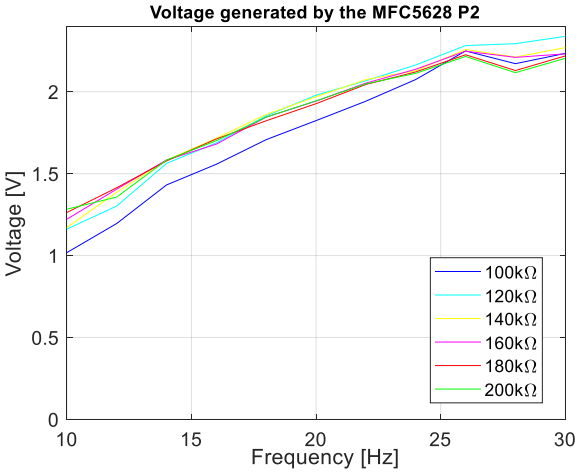

(c)

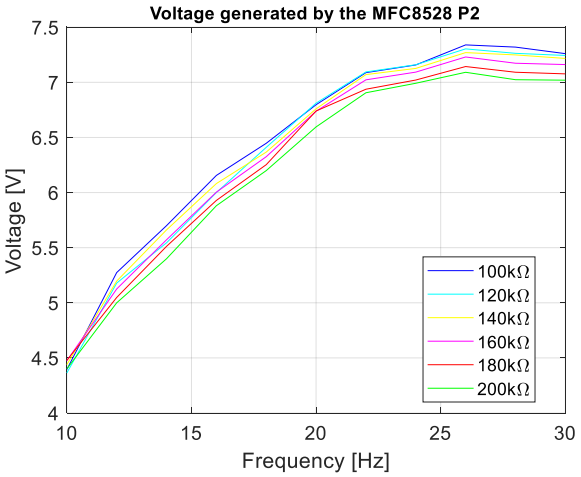

Fig. 7. Comparison of voltage generated by the real EH system with MFC of types (a) 8514 P2, (b) 5628 P2, (c) 8528 P2 by connecting them with resistive load in the range 100–200 kΩ

In addition, the lab stand was retrofitted into the system acquisition data National Instrument PXI used to measure the voltage generated by the EH system, as well as a laser displacement sensor LQ10A65PUA (Turck) to monitor the base acceleration. The lab stand, presented in Fig. 6, was also equipped with the signal generator Agilent and the vibration shaker TV51110-M with a BAA 120 amplifier (developed by Tira) to introduce a signal excitation.

In the first step, the experimental tests were carried out to measure the base acceleration and assess the power of the excitation signal. For this, an excitation signal in the form of a sinusoidal signal with an amplitude of 2 V and the frequency changing within the range of 10–30 Hz with a step of 1 Hz was generated from the signal analyser and later applied to the vibration shaker by an amplifier dedicated for this device. The displacement signal measured and recorded by using a laser sensor, which was placed in the distance of 4 mm from the vibrating base, was used to determine the value of the base acceleration (10 mm/s2–0.01 g) to ensure proper working of the proposed generator.

Next, the experimental tests were focused on matching the optimal impedance load connected to the EH system. For this, the optimisation process of the load resistance connected to the piezo was performed for six different resistive loads within the range of 100–200 kΩ with a step of 20 kΩ, as well as for three different types of MFC elements. The obtained results are shown in Fig. 7.

Fig. 7 indicates that the highest voltage is achieved for the matched resistance load equal to 120 kΩ. As a result, this impedance load can be called an optimal resistive load. Further analysis of the presented plots showed that the active area of the MFC significantly affected the amplitude of the voltage generated by the vibration-based energy harvesting system. This behaviour is shown in Fig. 7c, where using a piezo-strip with the highest active area generates the highest voltage amplitudes, which are close to 7.3 V. The inverse effect is achieved for the energy harvesting system with the piezo of the MFC 8514 P2 type, where a smaller width of this smart element leads to generating a voltage signal with the amplitude of only 1.1 V.

Next, the experimental tests were conducted to check how the frequency excitation influences the amplitude voltage generated by each piezo-composite attached to the flexure strip. For this, an experimental test was carried out for three different MFCs, where each of them was excited to vibration by applying a sinusoidal signal in the form of u(t) = 2sin(wt), with the frequency changing within the range of 10–30 Hz, and the resistive load was in the range of 100–300 kΩ.

(a)

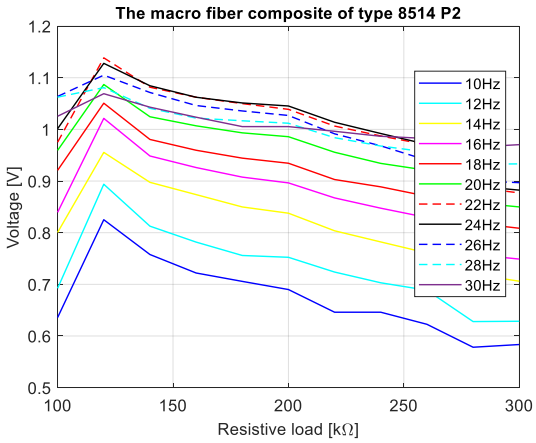

(b)

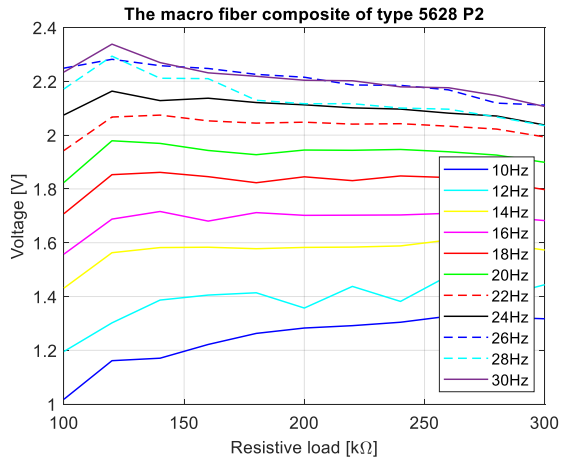

(c)

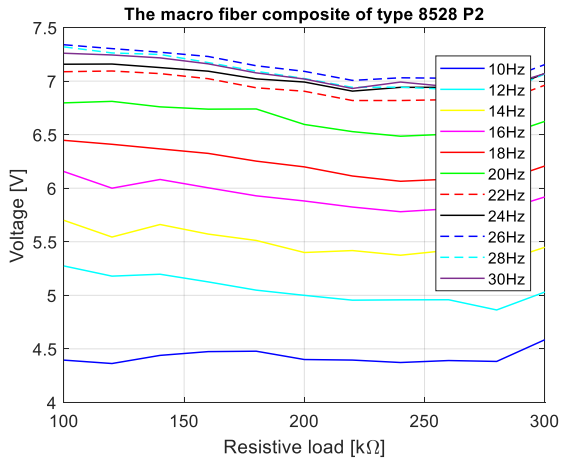

Fig. 8. Comparison of voltage generated by a real EH system with MFC of types (a) 8514 P2, (b) 5628 P2, (c) 8528 P2 excited to vibration with a frequency within the range of 10–30 Hz versus the resistive load

The results presented in Fig. 8 indicated that the highest voltage amplitude for each piezo-composite is generated for the micro-generator connected to the optimal resistive load set at 120 kΩ. This effect is shown in Fig. 8a and 8c, where an increase in the resistive load >120 kΩ for each considered excitation frequency led to a decrease in the voltage generated by the EH systems. Different results can be observed during the analysis of the energy harvesting with the piezo-composite of the MFC 5628 P2 type, where the amplitudes of voltages generated by this system were almost constant. This was due to smaller strains of the piezo of the 5628 P2 type, especially on the opposite edges.

Other experimental tests were carried out to check the power output generated by each considered piezo versus the load resistance connected to the piezo by various frequencies of excitation changing within the range of 10–30 Hz. The results presented in Fig. 9 indicate that the highest power output, which equals 0.5 mW, was achieved for the highest piezo of the MFC 8528 P2 type, while the lowest power output (12 μW) was achieved for the piezo-strip with the same length but twice the lowest width. As a result, it can be concluded that the width of the piezo-strip composite significantly affects the power output generated by the proposed micro-generator.

(a)

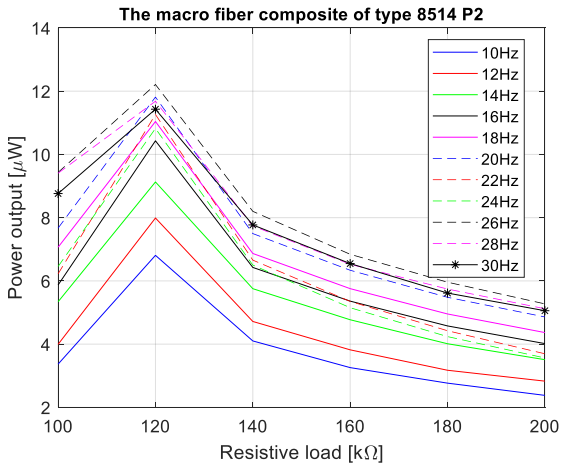

(b)

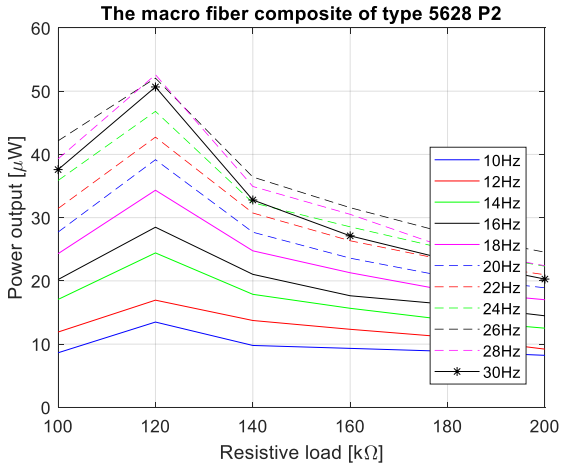

(c)

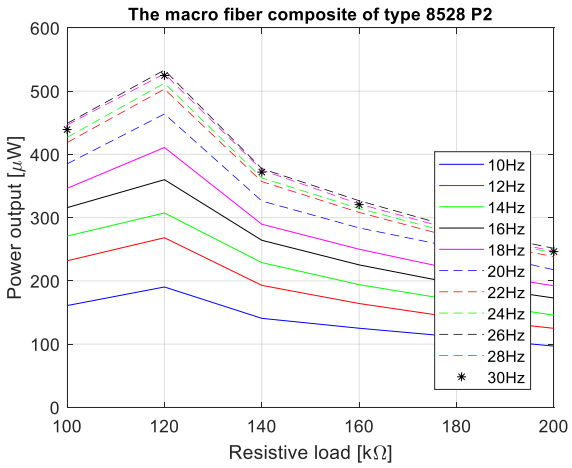

Fig. 9. Comparison of the power output generated by the EH system with an MFC of types (a) 8514 P2, (b) 5628 P2, (c) 8528 P2 excited to vibration with a frequency within the range of 10–30 Hz versus the resistive load

The last step of the experimental setup was to calculate the effectiveness of energy harvesting systems for three considered piezo-composites. To do this, firstly, the root mean square values for the obtained voltage output and excitation signals were calculated, and secondly, the power of these signals was determined.

$$\eta = \frac{P_{out}}{P_{in}} \cdot 100\% \tag{15}$$

DOI 10.2478/ama-2024-0026

where $\boldsymbol{P_{out}} = \boldsymbol{RMS(V_{out})^2} = \frac{1}{N}\sum_{i=1}^{N} \boldsymbol{V_{out}}^2$ is the power of the output voltage signal from the piezo harvester, $\boldsymbol{P_{in}} = \boldsymbol{RMS(u)^2} = \frac{1}{N}\sum_{i=1}^{N} \boldsymbol{u^2}$ is the power of the excitation harmonic signal.

(a)

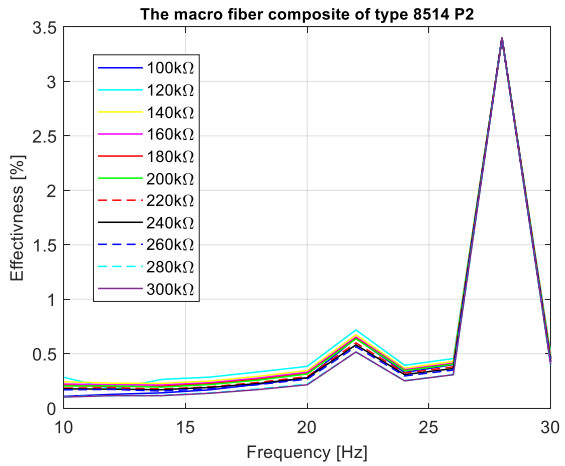

(b)

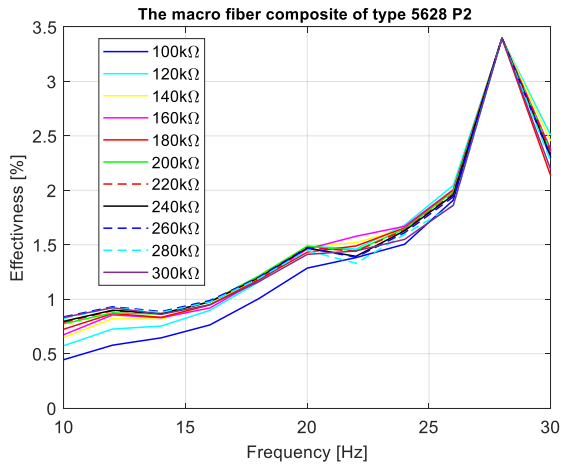

(c)

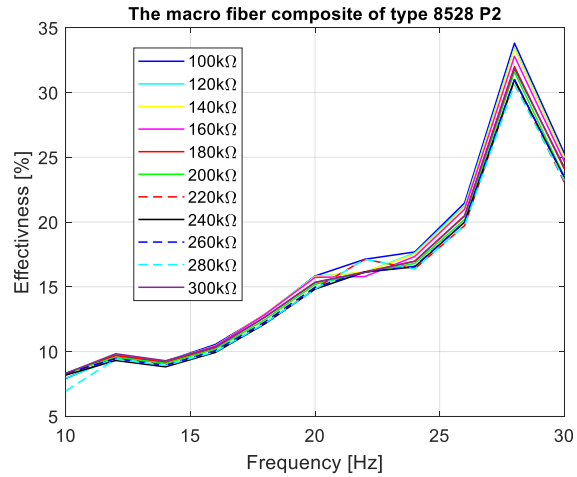

Fig. 10. Comparison of the effectiveness of a real EH system with a MFC of types (a) 8514 P2, (b) 5628 P2, (c) 8528 P2 by connecting them with the resistive load within the range of 100–300 kΩ

The obtained results presented in Fig. 10 indicated that the active area of the MFC attached to the flexure strip, as well as matched the resistive load of the energy harvesting system, plays an important role in enhancing the piezo generator efficiency. It is especially true for systems working at the resonance frequency, as well as around this frequency, where using the piezo-strip of the 8528 P2 type leads to increasing the effectiveness almost ten times (from 3.4% up to 33%). As a result, taking account of the results presented in other studies [30,33,34], it can be concluded that the proposed micro-power generator working with a frequency of 28 Hz can be a more useful device to power small electrical sensors with a low power demand, for example, to support the SHM system.

5. SUMMARY AND CONCLUSIONS

In this study, the effectiveness of the energy harvesting system located in the prototype of a micro-power generator for piezo-composites with different active areas was analysed. To this end, an FE model of the flexure strip with three different piezo-composites located symmetrically versus transverse axis of the flexure strip were analysed. The results obtained from numerical calculations (see Fig. 5) indicated that the proposed micro-generator with the piezo-composite of the 8528 type generates the highest amplitude of voltage, which is close to 7 V, while the voltage values are significantly lower for two other MFCs. This is due to the change in local strains of a particular piezo, which is >0.2 μm/mm for MFC 8528, while in the other case, it is <0.15 μm/mm.

Experimental tests of the EH system carried out on the lab stand, as shown in Fig. 6, for a real mechanical structure of the generator verified the numerical results. Again, the highest amplitudes of the voltage generated by the micro-piezo generator (see Fig. 7) were obtained for MFC 8528 P2, while the lowest values - for the piezo-composite with the same length but twice shorter width. As it was mentioned previously, the decrease in the voltage generated by the piezo of the 8514 P2 type is due to smaller local changes of the piezo strains.

In addition, the experimental tests were performed to determine the optimal resistive load, output power and effectiveness of the considered EH systems. The results presented in Fig. 8 show that the highest voltage amplitude for each piezo-composite was achieved by connecting the composite with the resistance load equal to R = 120 kΩ, further called the optimal resistive load, as well as by the frequency excitation close to the first natural frequency (fexc = 28 Hz). A similar effect was achieved by analysing the power output generated by particular piezo-composites. In this case again, the highest power value, close to 0.5 mW, was obtained for the piezo of the 8528 type. In other cases, the power generated by the EH system with the piezo-strip 5628 P2 and 8514 P2 types significantly decreased up to 50 μW and 12 μW, respectively, decreasing the effectiveness of the proposed micro-power generator from 33% to only 3.4% (see Fig. 10).

In sum, the obtained numerical and experimental results indicated that increasing the chosen geometrical parameters of the piezo-composite, such as length and width, leads to a significant increase in the voltage generated by the EH system. Therefore, the considered micro-piezo generator, when connected with a storing unit containing the optimal impedance load and a supercapacitor, can be used to power small electrical devices with a low

power demand. Hence, the current study filled the gap in the state of the art associated with the energy harvesting system with a homogenised material in the active layer of the MFC.

REFERENCES

1. Bradai S, Naifar S, Viehweger C, Kanoun O, Litak G. Nonlinear analysis of electrodynamics broadband energy harvester. European Physical Journal. Special Topics. 2015; 224: 2919-2927.
2. Chen Y, Yan Z. Nonlinear analysis of axially loaded piezoelectric energy harvesters with flexoelectricity. International Journal of Mechanical Science. 2020;173:105473.
3. Wang L, Yuan FG. Vibration energy harvesting by magnetostrictive material. Smart Mater Structures. 2008; 17(4).
4. Wei Ch, Jing X. A comprehensive review on vibration energy harvesting: Modelling and realization. Renewable and Sustinable Energy Reviews. 2017; 74: 1-18.
5. Dey S, Roy D, Patra S, Santra T. Performance of a modified magnetostrictive energy harvester in mechanical vibration. Heliyon. 2019; 5 (1).
6. Lei W, Yuang FG. Vibration energy harvesting by magnetostrictive material. Smart Material Structures. 2008; 17(4): 045009.
7. Lee CS, Joo J, Han S, Lee JH, Koh SK. Poly (vinylidene fluoride) transducers with highly conducting poly (3,4-ethylendioxythiopene) electrodes. Synthetic Metal 2005; 152(1-3): 49-52.
8. Morita T. Miniature piezoelectric motors, Sensors and Actuators. A: Physical. 2003: 103(3): 291-300.
9. Nicoletti R, de Araujo MVV. Electromagnetic harvester for lateral vibration in rotating machines. Mechanical Systems and Signal Processing. 2015:(52-53):685-699.
10. Wang I. Vibration Energy Harvesting by Magnetostractive Material for Powering Wireless Sensors. 2007. Doctoral Thesis.
11. Ouro-Koura H, Sotoudeh Z, Tichy JA, Borca-Tascius DA. Effectiveness of energy transfer versus mixing entropy in coupled mechanical-electrical oscillatiors. Energies. 2022;15:6105.
12. Roundy S, Wright PK, Rabaey J. A study of low level vibrations as a power source for wireless sensors node. Computer Comunications. 2013; 26(11): 1131:1144.
13. Li J, Ouro-Koura H, Arnow H, Nowbahari A, Galarza M, Obispo M, Tong X, Azadmehr M, Hella MM, Tichy JA, Borca-Tascius DA. A Novel comb design for enhanced power and bandwidth in electrostatic MEMS energy converters. IEEE 36th International Conference on Micro Electro Mechanical Systems (MEMS). DOI: 10.1109/MEMS49605.2023.10052590
14. Li J, Tichy J, Borca-Tascius DA. A predictive model for electrostatic energy harvesters with impact-based frequency up-conversion, Journal of Micromechanics and Microengineering. 2020; 30(12): 125012.
15. Li J, Ouro-Koura H, Arnow H, Nowbahari A, Galarza M, Obispo M, Tong X, Azadmehr M, Halvorsen E, Hella MM, Tichy JA, Borca-Tascius DA. Broadband Vibration-based Energy harvesting for Wireless Sensor Applications using Frequency Up-conversion. Sensors. 2023; 23(11): 5296.
16. Koszewnik A, Oldziej D. Performance assessment of an energy harvesting system located on a copter. European Physical Journa., Special Topics. 2019; 228: 1677–1692.
17. Koszewnik A. Analytical Modeling and Experimental Validation of an Energy Harvesting System for the Smart Plate with an Integrated Piezo-Harvester. Sensors. 2019; 19(4): 812.
18. Cahill P, Hazra B, Karoumi R, Mathewson A, Pakrashi V. Vibration energy harvesting based monitoring of an operational bridge undergoing forced vibration and train passage. Mechanical Systems and Signal Processing. 2018; 106: 265–283.
19. Na WS, Baek J. Piezoelectric Impedance-Based Non-Destructive Testing Method for Possible Identification of Composite Debonding Depth. Micromachines 2019, 10: 621.
20. O'Leary K, Pakrashi V, Kelliher D. Optimization of composite material tower for offshore wind turbine structures. Renewable Energy. 2019; 140: 928–942.
21. Okosun F, Cahill P, Hazra B, Pakrashi V. Vibration-based leak detection and monitoring of water pipes using output-only piezoelectric sensors. European Physical Journal Special Topics. 2019; 228: 1659–1675.
22. Koszewnik A. Experimental validation of equivalent circuit modeling of the piezo-stripe harvester attached to the SFSF rectangular plate. Acta Mechanica et Automatica. 2020; 14(1): 8-15.
23. Cahill P, Ni Nuallain NA, Jackson N, Mathewson A, Karoumi R, Pakrashi V. Energy Harvesting from Train-Induced Response in Bridges. Journal of. Bridge Engineering 2014; 19: 04014034.
24. Koszewnik A, Lesniewski K, Pakrashi V. Numerical Analysis and Experimental Verification of Damage Identification Metrics for Smart Beam with MFC elements to support structural health monitoring. Sensors. 2021; 21(20): 6796.
25. Ambroziak L, Ołdziej D, Koszewnik A. Multirotor Motor Failure Detection with Piezo Sensor. Sensors. 2023; 23(2): 1048.
26. Yang F, Gao M, Wang P, Zuo J, Dai J, Cong J. Efficient piezoelectric harvester for random broadband vibration of rail. Energy. 2021; 218: 119559.
27. Zheng J, Dou B, Li Z, Wu T, Tian H, Cui G. Design and Analysis of a While-Drilling Energy-Harvesting Device Based on Piezoelectric Effect. Energies. 2020; 14(5): 1266.
28. Wu Z, Xu Q. Design and Development of a Novel Two-Directional Energy Harvester with Single Piezoelectric Stack. IEEE Transaction and Industrial Electronics. 2021; 68: 1290–1298.
29. Kan J, Zhang M, Wang S, Zhang Z, Zhu Y, Wang J. A cantilevered piezoelectric energy harvester excited by an axially pushed wedge cam using repulsive magnets for rotary motion. Smart Material and Structures. 2021; 30: 065009.
30. Ju S, Ji Ch-H. Impact-based piezoelectric energy harvester. Applied Energy. 2018; 214: 139-151.
31. Zhou W, Penamalli GR, Zuo L. An efficient vibration energy harvester with a multi-mode dynamic magnifier. Smart Materials and Structures. 2012; 21: 015014.
32. Caban J, Litak G, Ambrozkiewicz B, Wolszczak P, Gardynski L, Stączek P. Impact-based piezoelectric energy harvesting system excited from diesel engine suspension. Applied Computer Science. 2020; 16(3): 16-29.
33. Peng Y, Xu Z, Wang, M, Li Z, Peng J, Luo J, Xie S, Pu H, Yang Z. Investigation of frequency-up conversion effect on the performance improvement of stack-based piezoelectric generators. Renewable Energy. 2021; 172: 551–563.
34. Wen S, Xu Q. Design of a Novel Piezoelectric Energy Harvester Based on Integrated Multistage Force Amplification Frame. IEEE/ASME Transaction Mechatronics. 2019; 24: 1228–1237.
35. Hwang GT et al. Self-powered wireless sensor node enabled by an aerosol-deposited PZT flexible energy harvester. Advanced Energy Materials. 2016; 6(13): 1-9.
36. Ramadoss A, Saravanakumar B, Lee SW, Kim YS, Kim SJ, Wang ZL. Piezoelectric-driven self-charging supercapacitor power cell. ACS Nano. 2015; 9(4): 4337-4345.
37. Gilshteyn EP et al. Flexible self-powered piezo-supercapacitor system for wearable electronics. Nanotechnology. 2018; 29(32): 1-14.
38. Pu X, Hu W, Wang ZL. Toward wearable self-charging power systems: the integration of energy-harvesting and storage devices. Small. 2018; 14(1): 1-19.
39. Zhao H, Wei X, Zhong Y, Wang P. A direction Self-tuning two-dimensional piezoelectric vibration energy harvester. Sensors. 2020; 20(77): 1–13.
40. Selleri G, Poli F, Neri R, Gasperini L, Gualandii Ch, Soavi F, Fabiani D. Energy harvesting and storage with ceramic piezoelectric transducers coupled with an ionic liquid-based supercapacitor. Journal of Energy Storage. 2023;60:106660.

41. Koszewnik A. The influence of a slider gap in the beam-slider structure with an MFC element on energy harvesting from the system: experimental case. Acta Mechanicca. 2021;232: 819-833.
42. Ma Y, Wang J, Lic Ch, Fu X. A micro-power generator based on Two Piezoelectric MFC Films. Crystals. 2021; 11(8): 861.
43. Hu K, Li H. Large deformation mechanical modeling with bilinear stiffness for Macro-Fiber Composite bimorph based on extending mixing rules. Journal of Intelligent Material Systems and Structures. 2020; 1-13. DOI:10.1177/1045389X20951257

The author acknowledges the funding from the commissioned task entitled "VIA CARPATIA Universities of Technology Network named after the President of the Republic of Poland Lech Kaczyński", contract no. MEiN/2022/DPI/2577 action entitled "In the neighborhood - inter-university research internships and study visits."

.

Andrzej Koszewnik: https://orcid.org/0000-0001-6430-6007